Enhancing visible-light photocatalytic activity by strongly binding flake $BiFeO_3$ nanoparticles on graphene sheets

Ying Huang ✉, *Yuanyuan Shen, Xiulan Qin, Ke Wang*

Department of Applied Chemistry and The Key Laboratory of Space Applied Physics and Chemistry under Ministry of Education, School of Science, Northwestern Polytechnical University, Xi'an 710072, People's Republic of China
✉ *E-mail: yingh@nwpu.edu.cn*

Published in Micro & Nano Letters; Received on 27th August 2019; Revised on 26th February 2020; Accepted on 17th June 2020

To investigate the influence of graphene on the photocatalytic activity of bismuth ferrite ($BiFeO_3$), $BiFeO_3$ and flaky $BiFeO_3$@graphene were prepared through the hydrothermal-synthesis process. The as-prepared particles were characterised by XRD, TGA, SEM, X-ray photoelectron spectroscopy, and PL measurements. The results show that the $BiFeO_3$ nanoparticles have a microstructure and homogeneously attached to graphene sheets. Moreover, the flaky $BiFeO_3$@graphene composites exhibited higher photocatalytic efficiency than pure $BiFeO_3$, especially under visible light irradiation. The synergistic effects of graphene and $BiFeO_3$ of composites were proposed to guide the further improvement of their photocatalytic activity.

1. Introduction: Photocatalytic materials have attracted considerable attention over the past decade due to world-wide environmental issues, especially to purify polluted wastewater and/or split water for hydrogen production [1, 2]. Bismuth ferrite ($BiFeO_3$) is considered as one of the several single-phase room-temperature multiferroic materials with rhombohedral structure [3]. Recently, it has been shown that $BiFeO_3$ is an effective visible-light-driven photocatalyst due to its chemical stability, narrow band gap (2.5 eV) and low cost [4]. However, the fast recombination rate of electrons and holes, the low visible light absorption, and the low quantum efficiency make the $BiFeO_3$ photocatalysts far away from practical use.

To mitigate the above intractable problems, numerous researchers have been focused on the improvement of $BiFeO_3$ by doping elemental for band engineering, changing in the morphology of particles, as well as by preparing nanocomposites. Among various methods, preparing graphene-photocatalyst composites is more attractive, since its outstanding properties, such as excellent electron-transport property and 2D geometry [5]. Besides that, the photo-generated electron–hole pairs can be fast separated by graphene capturing the photo-generated electrons, which leads to an increased lifetime of the electron–hole pair photo-generated.

In this Letter, the flaky $BiFeO_3$@graphene composites were prepared by a facile hydrothermal method, in which $BiFeO_3$ nanocrystallites were directly synthesised on the graphene nanosheets. The photocatalytic activities of prepared samples were evaluated by the degradation of methylene orange (MO) under simulated sunlight irradiation.

2. Experimental method

2.1. Sample preparation: Synthesis of flake $BiFeO_3$@graphene composites: graphene oxide (GO) was synthesised using modified Hummer's method as reported earlier [6]. Precursors of $BiFeO_3$ were then prepared by a reverse co-precipitation method, appropriate amounts of $Bi(NO_3)_3{\cdot}5H_2O$ and $Fe(NO_3)_3{\cdot}9H_2O$ were used as starting materials and were dissolved in HNO_3 solution. The solution was added slowly drop-by-drop into ammonia solution under vigorous stirring. After that, the precipitants were washed with DI water several times to obtain the precursors. For the preparation of flake $BiFeO_3$@graphene composites, GO and the precursors of $BiFeO_3$ were dispersed in ultrapure water by ultrasonication, simultaneously. Then KOH (2, 4, 6, and 8 M) was successively added slowly into the aqueous solution and stirred for 30 min. Finally, the hybrid complex was transferred into a 100 ml sealed Teflon-lined autoclave for 12 h at 200°C. Finally, the product then was separated, washed several times with ethanol, and dried at 60°C for 12 h. (The process is schematically illustrated in Fig. 1.) The bare flaky $BiFeO_3$ was synthesised under the same condition.

2.2. Materials characterisation: The phase of the prepared samples was characterised by XRD analysis (Rigaku, model D/max-2500 system at 40 kV and 100 mA of Cu Kα). Thermal analysis of the composite was done by TGA (Model Q50, TA, USA) under an air atmosphere, with a heating rate of 20°C /min, and the temperature range was from 20 to 800°C. X-ray photoelectron spectroscopy (XPS) analysis was conducted by an X-ray photoelectron spectrometer (Al K-Alpha; Thermo Fisher Scientific, USA). The surface morphology of the composites was performed by SEM (SuPRA 55, German ZEISS).

The photo-induced decomposition of MO was carried out with 10 mg of catalyst suspended in MO solution with an initial concentration of 10 mg/l (80 ml) under the irradiation of 55 W visible light lamp (an optical filter was used to cut-off the ultraviolet (UV) light (λ<400 nm) in front of the Xenon lamp). Prior to irradiation, the suspensions are sonicated in the dark for 20 min to ensure the establishment of adsorption/desorption equilibrium. At the given time interval, 4 ml suspension is withdrawn and centrifuged. The absorption spectra of the solution are determined using a UV/Visible spectrometer. The degradation efficiency was evaluated by the function of C_t /C_0, where C_0 is the initial concentration of MO and C_t is the concentration after degradation.

The sample was dispersed into MO aqueous solution with a concentration of 5 mg/l, and kept in the dark for 12 h to establish adsorption/desorption equilibrium. An optical filter was used to cut-off the UV light (λ < 400 nm) in front of the Xenon lamp, and irradiation lasted 5 h under continuously stirring. The reaction solution was periodically taken from the reactor for the determination of the absorbance change. The concentration variation of MO was obtained according to the concentration absorbance (at 664 nm) relationship.

3. Results and discussions: To obtain deep insight into the structure of the synthesised samples, XRD patterns of samples synthesised at different KOH concentrations of 2, 4, 6, and

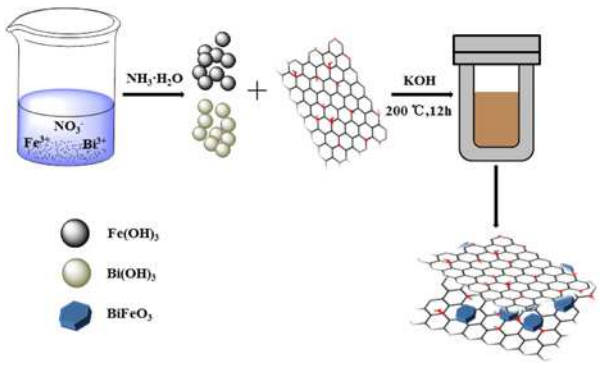

Fig. 1 *Schematic illustration of fabrication process for flaky $BiFeO_3$@graphene composites*

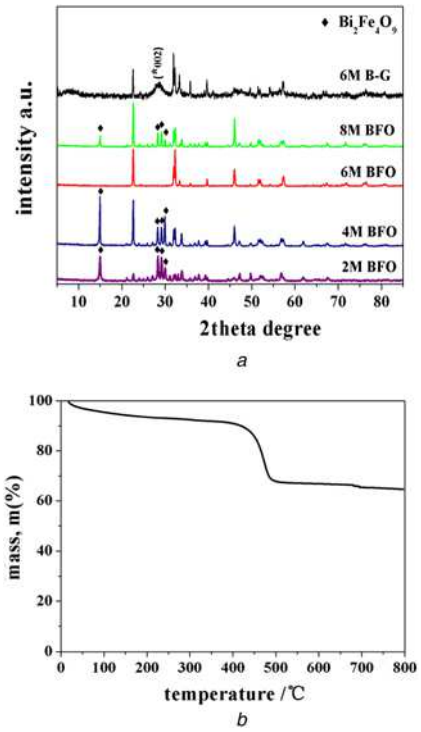

Fig. 2 *Physical parameters of the $BiFeO_3$@graphene composites*
a XRD patterns of flaky $BiFeO_3$ under different concentration of mineraliser (2, 4, 6, and 8 M) and flaky $BiFeO_3$@graphene composites
b TGA curve of flaky $BiFeO_3$@graphene composites

8 mol l^{-1} and flaky $BiFeO_3$@graphene composites synthesised at 6 mol l^{-1} were performed in Fig. 2*a*. It is evident from XRD patterns that the product is in pure $BiFeO_3$ crystal phase (JCPDS 86-1518) when KOH concentration is 6 mol l^{-1}. It can be found that $Bi_2Fe_4O_9$ phase appears as KOH concentration is 2, 4, 8 mol L^{-1}, which could be understand by the difference between the solubility of ferric ion and that of bismuth ion in the solution when KOH concentration is lower or higher than 6 mol L^{-1}. All the identified peaks of the flaky $BiFeO_3$@graphene composites show sharp diffraction peaks, which can be indexed as those of $BiFeO_3$. Furthermore, the characteristic diffraction peak of the GO (*002) confirms the presence of graphene in the composite. The results indicate that the graphene coating has no influence on the crystal structure of $BiFeO_3$. To eliminate the content of graphene, the thermogravimetric tests of the flaky $BiFeO_3$@graphene composites were continuously heated from 25 to 800°C in an air atmosphere. As shown in Fig. 2*b*, the weight loss before 100°C is due to the release of absorbed water.

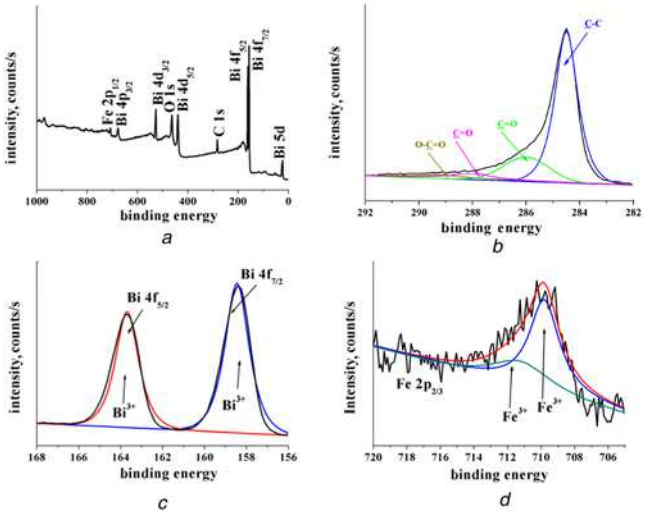

Fig. 3 *XPS spectra of*
a Survey scan
b C 1s of graphene
c Bi 4f spectrum
d Fe 2p spectrum

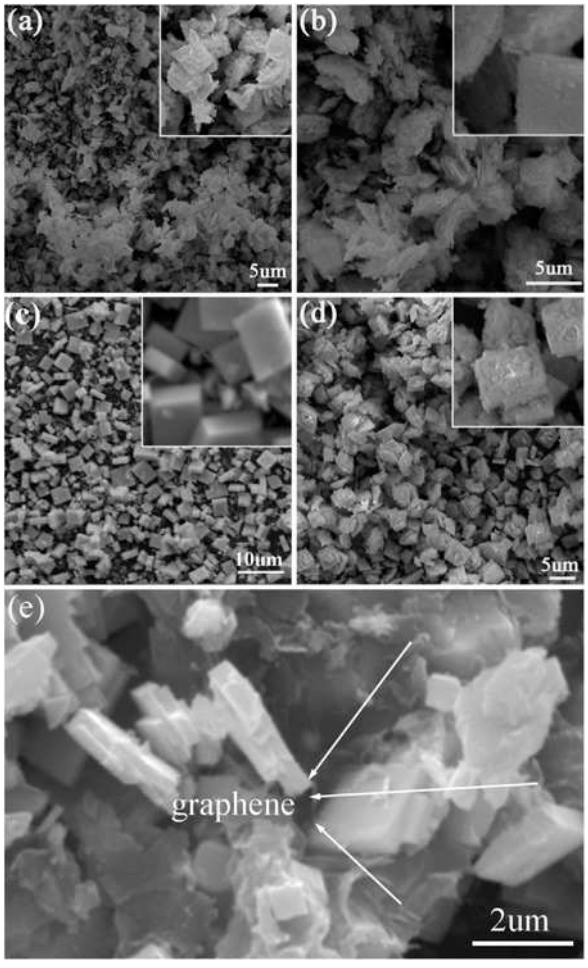

Fig. 4 *SEM images of*
a–d Flaky $BiFeO_3$ under different concentration of mineraliser (2, 4, 6, and 8 M)
e Flaky $BiFeO_3$@graphene composites

The notable weight loss occurring between 200 and 700°C is ascribed to the combustion of C-groups due to C-group oxidation. Therefore, according to the change of weight, it is estimated that the

doi: 10.1049/mnl.2019.0515

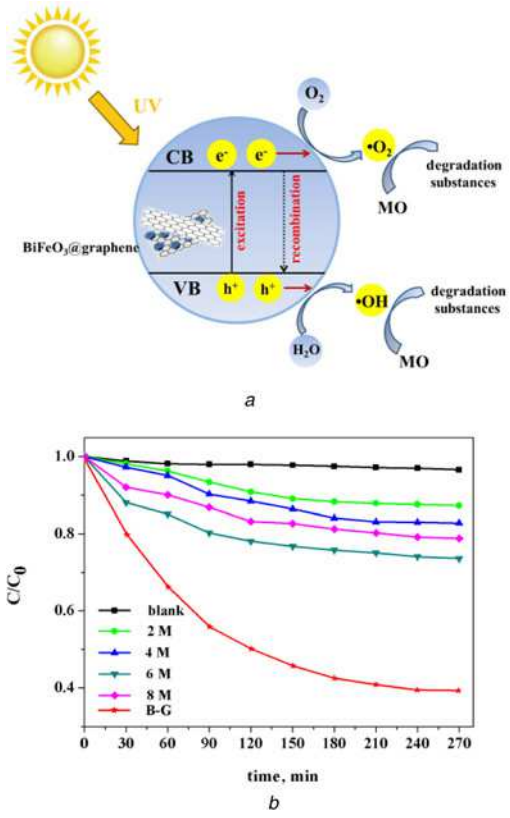

Fig. 5 *Results of MO photodegradation*
a Schematic illustrating photocatalytic mechanism of $BiFeO_3$@graphene during degradation of MO
b Results of MO photodegradation: flaky $BiFeO_3$ under different concentrations of mineraliser (2, 4, 6, and 8 M) and flaky $BiFeO_3$@graphene composites

amount of flaky $BiFeO_3$ and graphene in the composites is 69.4% and 30.6 wt%, respectively.

The XPS analysis was used to further study the surface chemical composition of synthesised flaky $BiFeO_3$@graphene composites. Fig. 3*a* shows the full XPS spectrum of composites, it is obvious that the presence of the Bi 4f peak at 158.6 and 164.2 eV, C 1s peak at 284 eV, O 1s peak at 529.5 eV, and Fe 2p peak at 710.2 eV can be observed in the wide scan XPS spectrum. As shown in Fig. 3*b*, the C 1s peak in the high-resolution XPS spectrum consists of four peaks. The fitted different peaks at 284.5, 287.5, 288.6, and 289.1 eV correspond to C–C bonding, C–O, C=O and O–C=O, respectively [7, 8]. Two peaks of the Bi element were noted in the curve. The strong peaks at 158.6 and 164.2 eV for Bi^{3+} were Bi 4f $_{7/2}$ and Bi 4f $_{5/2}$, respectively, which is present in Fig. 3*c*. As shown in Fig. 3*d*, two peaks of the Fe element are obviously observed at a binding energy of 710.2 eV and they can be signed to Fe^{3+}. The presence of multiplets indicates that Fe may have two kinds of coordination states [9].

Fig. 4 shows the morphology of the as-prepared bare $BiFeO_3$ under different concentrations of mineraliser (2, 4, 6, and 8 M) and flaky $BiFeO_3$@graphene composites. It is evident from the SEM images that the morphology changes from irregular agglomeration to regular polyhedron with increasing the KOH concentration. The powders dominated by the $Bi_2Fe_4O_9$ phase are composed of nanoflakes (Fig. 4*a*) at lower KOH concentration. With the concentration of KOH was increased to 4 M, the morphology of the synthesised particles changes from nanoflakes to self-assembled particles (Fig. 4*b*), corresponding to the evolution of the dominant phase from $Bi_2Fe_4O_9$ to $BiFeO_3$. When the KOH concentration was adjusted to 6 M, the $BiFeO_3$ crystals mainly exhibit regular morphology, which is shown in Fig. 4*c*. However, continued to increase the KOH concentration to 8 M, the surfaces of particles become rough and grow to small trigonal facets (Fig. 4*d*). Therefore, uniform and regular flaky $BiFeO_3$ were successfully obtained through controlling the KOH concentration at 6 M. The microstructure of the flaky $BiFeO_3$@graphene composites is shown in Fig. 4*e*. As shown in images, flaky $BiFeO_3$ are successfully deposited onto the surfaces of graphene sheets. This result indicates that the bare $BiFeO_3$ deposited on graphene sheets can also prevent themself from stacking into multilayers.

The degradation of organic pollutants by photocatalysts is believed to be controlled by free-radical chemistry. The electron–hole pairs excited by light irradiation can activate both O_2 and H_2O to form various kinds of reactive species, such as ·OH and $\cdot O_2^-$, shown in Fig. 5*a*. These reactive species are expected to have an ability to decompose different organic pollutants by distinct reaction pathways during the subsequent reactions [10]. The photodegradative activity of MO on flaky $BiFeO_3$ and flaky $BiFeO_3$@graphene composites is shown in Fig. 5*b*. As is shown, the degradation rate of MO is <3% without using $BiFeO_3$ nanoparticles as the catalyst even after 270 min visible-light irradiation ($\lambda > 420$ nm of Xe lamp), indicating that MO is a stable pollutant. In addition, all the flaky $BiFeO_3$ have visible-light-induced photocatalytic activities and the sequence of photocatalytic efficiency is 6 M $BiFeO_3$ > 8 M $BiFeO_3$ > 4 M $BiFeO_3$ > 2 M $BiFeO_3$. The flaky $BiFeO_3$ obtained at KOH concentration of 6 M exhibits better photocatalytic activity than other samples. The results indicate that the $Bi_2Fe_4O_9$ phase when KOH concentration is lower or higher than 6 mol l^{-1}, the $Bi_2Fe_4O_9$ phase appears, which has a negative influence on photocatalysis efficiency.

4. Conclusion: In summary, the flaky $BiFeO_3$@graphene composites are successfully prepared through the hydrothermal-synthesis process to use visible light more effectively in photocatalytic reactions. The existence of bonding between $BiFeO_3$ and graphene is characterised by XPS analysis. These advantages combined with the large intrinsic charge mobility of graphene give rise to a much enhanced photocatalytic performance of flaky $BiFeO_3$@graphene composites. Above all, the superior visible light response of these flaky $BiFeO_3$@graphene composites makes them promising candidates as advanced photocatalysts in the visible range.

5. Acknowledgment: The research was supported by the National Natural Science Foundation of China (51872236).

6 References

[1] Zhou P., Yu J.G., Jaroniec M.: 'All-solid-state Z-scheme photocatalytic systems', *Adv. Mater.*, 2014, **26**, (29), pp. 4920–4935
[2] Wang H., Feng H.B., Li J.H.: 'Graphene and graphene-like layered transition metal dichalcogenides in energy conversion and storage', *Small*, 2014, **10**, (11), pp. 2165–2181
[3] Huo Y., Jin Y., Zhang Y.: 'Citric acid assisted solvothermal synthesis of $BiFeO_3$ microspheres with high visible-light photocatalytic activity', *J. Mol. Catal. A, Chem.*, 2010, **331**, (1), pp. 15–20
[4] Zhu A., Zhao Q., Li X., *ET AL.*: '$BiFeO_3/TiO_2$ nanotube arrays composite electrode: construction, characterization, and enhanced photoelectrochemical properties', *ACS Appl. Mater. Interfaces*, 2014, **6**, pp. 671–679
[5] Zhang N., Zhang Y., Xu Y.J.: 'Recent progress on graphene-based photocatalysts: current status and future perspectives', *Nanoscale*, 2012, **4**, (19), pp. 5792–5813
[6] Wang K., Xu Y, Li Y., *ET AL.*: 'Sodium storage in hard carbon with curved graphene platelets as the basic structural units', *J. Mater. Chem. A*, 2019, **7**, pp. 3327–3335
[7] Qin X., Huang Y., Wang K., *ET AL.*: 'Novel hierarchically porous Ti-MOFs/nitrogen-doped graphene nanocomposite served as high

efficient oxygen reduction reaction catalyst for fuel cells application', *Electrochim. Acta*, 2019, **297**, pp. 805–813

[8] Jaiswal A., Das R., Vivekanand K., *ET AL.*: 'Effect of reduced particle size on the magnetic properties of chemically synthesized $BiFeO_3$ nanocrystals', *J. Phys. Chem. C*, 2010, **114**, (5), pp. 2108–2115

[9] Wu L., Li J., Dong C., *ET AL.*: 'Exploring origin of ferromagnetism from abnormal exchange bias in Mn-doped $BiFeO_3$ nanoparticles', *Sci. Adv. Mater.*, 2014, **6**, (9), pp. 1943–1950

[10] Pradeep Reddy Vanga R.V., Ashok M.M.: 'Structural, magnetic and photocatalytic properties of La and alkaline co-doped $BiFeO_3$ nanoparticles', *Mater. Sci. Semicond. Process.*, 2015, **40**, pp. 796–802

doi: 10.1049/mnl.2019.0515